

WORKING PAPER 340

REMOTE SENSING OF SOIL MOISTURE (2) :

THE THERMAL INFRARED WAVELENGTHS

JOHN COYLE

---

**WORKING PAPER**  
**School of Geography**  
**University of Leeds**

### Abstract

Estimates of the moisture content of near-surface soils can be made from remotely sensed data collected from aircraft and spacecraft. Existing techniques which make use of data collected at thermal infra-red wavelengths are reviewed. The terrestrially emitted radiation which is measured by a radiometer is closely related to earth surface temperature. Surface temperature is, in turn, an integral response to the energy exchanges between the soil, the vegetative canopy and the atmosphere. Thermal models based on these processes and concepts such as the soil-plant-atmosphere continuum are discussed.

Remote Sensing of Soil Moisture (2)The Thermal Infrared WavelengthsContents

	Page
(1) General Introduction	2
(2) The Thermal Infrared Wavelengths (Introduction)	5
(3) Radiation and Temperature	6
(4) Thermal Models of the Earth's Surface	10
(4.1) Transport Equations and Boundary Conditions	10
(4.2) The Algorithms	16
(4.3) Numerical Models	19
(4.4) Analytical Models	25
(4.5) Summary and Discussion of Section 4	28
(5) The Problem of Vegetation	31
(6) General Discussion	37
(7) References	42
(8) Diagrams	

Remote Sensing of Soil Moisture.(1). General Introduction

There is a growing need for frequent and accurate estimates of the moisture content of surface soils. This need may be identified at various levels ranging from local and regional scales to a national scale. It is felt most keenly by scientists working within the hydrological, agricultural and meteorological sciences. In these, estimates of soil moisture are crucial for modelling and planning of natural resources. For example, agricultural scientists might use estimates of soil moisture to predict crop growth and yields whilst hydrologists may use such estimates for managing water supply based on integrated models for watershed planning. It is not surprising, therefore, to find that the estimation of soil moisture has provided a focus for research for many scientists in recent years.

Conventional techniques of measuring the moisture content of surface soils suffer from two major limitations. The first of these relates to the physical disturbance of the soil by the measurement technique itself. For example, the gravimetric techniques express soil moisture as the volumetric water content of a sample of soil taken from a site. During the process of measurement, the water regime of the soil is disturbed. This tends to give rise to large errors in measurement and to limit the usefulness of the method, especially if one is attempting to monitor changes in soil

moisture over a long period of time. More advanced techniques based on neutron scattering, gamma ray attenuation or electric current flow within the soil, are subject to the same limitation although they generally avoid the need to take samples from the soil body (McKim *et. al.* 1980).

The second limitation relates to the high density of sampling points needed to obtain accurate estimates of soil moisture over large areas using conventional techniques. An adequate sampling density is rarely achieved because of the high cost of field observations. Estimates of soil moisture content over large areas are therefore limited in accuracy due to the large interpolations which have to be made between points. These may leave out many important features such as pockets of saturated soil (Elkington, 1979).

The measurement of soil moisture from space or airborne platforms offers a solution to these problems. Remote sensing techniques have a good potential for providing timely and comprehensive areal coverage with few of the problems of limited accessibility or sampling density of the more traditional methods of soil moisture measurement.

Several techniques have been devised for the purpose of extracting soil moisture information from remote sensor data. These fall into three broad categories based on the region of the electromagnetic spectrum within which they operate. These are:

- (1) The visible and reflective infrared waveband (0.38 $\mu$ m-3.0 $\mu$ m).
- (2) The thermal infrared waveband (3.0 $\mu$ m-15.0 $\mu$ m).
- (3) The microwave waveband (0.1 to 300 cm)

This paper deals with the remote sensing of soil moisture within the thermal infrared portion of the electromagnetic spectrum. A brief outline of the physical principles together with a review of the literature dealing with soil moisture estimation at these wavelengths is given. Complementary papers dealing with the remote sensing of soil moisture in the other two wavebands are also available.

## (2). The Thermal Infra-red Wavelengths

### Introduction

The intensity of the terrestrial radiation spectrum is greatest between the wavelengths of  $3\mu\text{m}$  and  $15\mu\text{m}$ . This wavelength band is known as the thermal infra-red. Remote sensing in this region of the electromagnetic spectrum is fundamentally different from its counterpart in the visible and reflective infra-red. The latter is based almost entirely on reflected solar energy and the intensity of thermal infra-red radiation in the solar spectrum is low. There is a close relationship between the radiative characteristics of the earth and its temperature. Remote sensing at thermal infra-red wavelengths thus allows the surface temperature of the earth to be monitored. From this data, knowledge of surface geology and the water and agricultural resources of the earth may be gained. The following chapter describes some of the physical principles behind the thermodynamic behaviour of the earth's surface and their use in the interpretation of thermal infra-red data. Again concentration is given to the remote sensing of soil moisture.

(3). Radiation and Temperature

An atom of any element may absorb or emit energy through a discrete change in its electronic state. The idea that energy is absorbed and emitted in this quantum fashion was first put forward as a rigorous theory by Max Planck in 1901. If an electron moves from quantum energy level ( $\mathcal{E}_1$ ) to a lower quantum energy level ( $\mathcal{E}_2$ ), then the frequency ( $f$ ) of the emitted radiation is given by Bohr's equation; (Ulaby et. al., 1981).

$$(1) \quad f = (\mathcal{E}_1 - \mathcal{E}_2) / h$$

where  $h$  is Planck's constant. Absorption of energy is manifested as change from a lower energy state to a higher energy state. The discrete nature of emission and absorption by individual atoms explains the characteristic line spectra of atomic gases.

The energy status of molecules is slightly more complex. Due to their greater mass, the energy represented by the vibrational (and to a lesser degree rotational) movement of molecules relative to each other reaches a degree of magnitude which exceeds the energy represented by a quantum jump from one electronic state to another. The number of quantised energy states also becomes much greater. Thus the absorption spectra of common atmospheric gases such as carbon dioxide and ozone tend to approximate to continuous bands of wavelengths rather than to several discrete line spectra. For



solids the degree of freedom to move from one energy state to another is so great that emission and absorption of radiation is observed to be continuous over all wavelengths (Reeves, 1975). The probability of a molecule emitting radiation is governed by the probability of its collision with a neighbouring molecule. The probability of collision increases with the amount of random vibrational movement which, by definition, is measured as the temperature of the substance. Thus the spectrum and intensity of radiation emitted by a target is directly related to its temperature (see Fig. 1). This forms the basis of remote sensing at thermal infra-red wavelengths.

The irradiance ( $E$ ) emitted by a target, integrated over all wavelengths, is given by the Stefan-Boltzmann law ;

$$(2) \quad E = \sigma \epsilon T^4$$

where  $T$  is the thermodynamic temperature,  $\sigma$  is the Stefan-Boltzmann constant and  $\epsilon$  is the emissivity of the target. For a perfect "black-body" radiator, the emissivity  $\epsilon$  is unity. Although there are few perfect radiators in nature, many surfaces approximate to black-body behaviour. In the thermal infra-red band (3 $\mu$ m to 15 $\mu$ m), the emissivity of exposed soils, for example, commonly ranges from 0.95 to 0.97 (Taylor, 1979).

The sun approximates to a black-body with a temperature of just under 6000°K. Passive remote sensing in the visible and reflective infra-red portions of the solar emitted spectrum operates at wavelengths where the intensity of

reflected radiation (after atmospheric attenuation) is greatest. Passive remote sensing at thermal infra-red wavelengths uses the peak intensities of terrestrial, emitted radiation ( $3\mu\text{m}$  to  $15\mu\text{m}$ ) which is characteristic of a black-body temperature of about  $300^\circ\text{K}$ . (see Fig 1). Remote sensing at these wavelengths is therefore based on the thermal and emissive properties of the earth's surface rather than on its reflective properties as is the case at visible wavelengths. The emissive properties of the earth's surface are relatively stable at thermal infra-red wavelengths although they can introduce error if not accounted for. The thermodynamic temperature of the surface, its spatial and temporal variation, is therefore the major source of information about the nature of the surface.

Since surface temperature is an integral response by a surface to environmental factors (including insolation, evaporation, transpiration, albedo, the thermal properties of the underlying soil, etc.), it offers a good potential for measuring, more or less indirectly, any one of these factors. For the same reason, however, a surface temperature value does not uniquely define a value for any of these same variables. A quantitative assessment of the complete energy and moisture fluxes at the earth's surface is required for unambiguous interpretation of the temperature of a surface.

A classification of the variables needed for the interpretation of radiometric temperatures is shown in Table 1. 'Radiometric temperature' refers to the apparent temperature of the earth's surface as measured by a radiometer

without any correction for surface emissivity (i.e. emissivity is assumed to be equal to unity).

Becker (1980) classified these variables into two groups, viz. useful and perturbative. Which variables belong to which group is dependent on the phenomena of interest. In soil moisture investigations, the atmospheric and topographic variables are clearly perturbative, as are variations in surface emissivity, since these factors can distort the one-to-one relationship between thermodynamic temperature and radiometric temperature.

Although the exact details of the energy exchange mechanisms at the earth's surface remain elusive (Green and Harding, 1979), the basic principles behind these exchanges have been known for some time (Pratt and Ellyet, 1978). Consequently most of the research involving these interactions continues to be concerned with the development of more efficient algorithms to extract soil moisture, evapotranspiration and thermal inertia values from remotely sensed data in the  $8\text{ }\mu\text{m}$  to  $12\text{ }\mu\text{m}$  wavelength band.

#### (4). Thermal Models of the Earth's Surface

All thermal models are basically the same (Rosema, 1976).

They consist of:

- (a) Transport equations and boundary conditions
- (b) An algorithm solving these equations.

These are considered in turn.

##### (4.1) Transport equations and boundary conditions.

Thermal energy may be transported through a soil either by conduction between the various soil layers or by the passage of soil moisture which is the most mobile of soil constituents. The latter process is only of importance in the case of vapour movement along a thermal gradient in very dry soils (Fig. 5(b)). The main effect of moisture, however, is to alter the thermal behaviour of soils. Water has a greater specific heat capacity ( $4 \text{ kJ kg}^{-1} \text{ K}^{-1}$ ) than most other soil constituents (the value for quartz is  $0.8 \text{ kJ kg}^{-1} \text{ }^{\circ}\text{K}^{-1}$ ) and its thermal conductivity is a degree of magnitude greater than the air it replaces within the soil matrix on wetting. Thus an increase in soil moisture content has the overall effect of stabilising the temperature fluctuations of a soil which is exposed to a periodically varying radiation source such as the diurnal variation between solar radiation receipt and emitted longwave radiation. The remote sensing of soil moisture in the thermal infra-red band is based on the inverse of this situation, that is, the inference of moisture content from the diurnal temperature wave of the soil surface (Fig 2).

A different suite of processes (evaporation, convection, radiation, etc.) operates between the surface and the atmosphere. The balance of these at the soil-atmosphere interface forms the upper boundary condition for the solution of the equations which describe the transport of heat and moisture through a soil. The assumption that heat and moisture flux at depth is negligible or has reached a steady state condition forms the lower boundary conditions. The transport equations are:

(a) The heat transport equation

The conduction of heat through a solid, homogeneous body is described by the Fourier equation. Assuming isotropic conditions in the horizontal plane, the heat flux ( $Q$ ) in the vertical plane is given by;

$$(3) \quad Q = \lambda \, dT/dz$$

where  $\lambda$  is the thermal conductivity of the medium and  $T$  is the temperature at depth  $z$ . Equation (3) holds instantaneously and for steady state conditions. In the field, soil temperatures rarely achieve such an equilibrium (Marshall and Holmes, 1979). Through a consideration of the conservation of energy within a unit volume of material, the following relationship is derived (Watson, 1979):

$$(4) \quad - \frac{\partial Q}{\partial z} = \rho c \frac{\partial T}{\partial t}$$

Combining equations (3) and (4) , the general equation for the conduction of heat through a body with thermal conductivity  $\lambda$  and volumetric heat capacity ( $\rho c$ ) is obtained:

$$(5) \quad \frac{\partial T}{\partial t} = \left( \lambda / \rho c \right) \frac{\partial^2 T}{\partial z^2}$$

The quantity ( $\lambda / \rho c$ ) is often abbreviated to (K), the thermal diffusivity. In a heterogeneous material like soil, thermal conductivity ( $\lambda$ ) and volumetric heat capacity ( $\rho c$ ) are dependent on the constituents of the soil, which vary spatially and with depth (z), and, in the case of soil moisture, on a time scale ranging from hours to days. If a model is designed to evaluate the heat flux within a soil for the purposes of estimating its soil moisture content, then additional information regarding the physical properties of the soil is required.

There are several possible sources of soil information which may be used in conjunction with a remote sensing system, given a requirement for comprehensive areal coverage. Soil survey reports, for example, are available for selected 100 km areas of Scotland, Wales and England. (e.g. Harrod, 1978). Unpublished information for wide areas other than those covered by soil survey reports is also held by organisations such as the Soil Survey for England and Wales and construction companies. Although properties such as thermal conductivity, moisture diffusivity, etc., are not explicitly stated in these reports, they may be calculated from the soil mineral fractions (% sand, silt, clay) by the methods of De Vries and

Van Wijk (1966). The volumetric heat capacity ( $\rho c$ ), for example, may be derived from:

$$(6) \quad \rho c = \sum \theta_i (\rho c)_i$$

where  $\theta_i$  is the volumetric fraction of constituent  $i$  in the soil. Problems with soil survey data include those of inappropriate scale, incomplete coverage, the subjective nature of soil property assessment in the field and the varying classification procedures. The English system (Avery, 1973), for example, emphasises soil drainage conditions whereas the U.S. system is based largely on criteria of climatic moisture and temperature regimes, reflecting respectively the agricultural problems and size of each country (Butler, 1980). Despite these problems, Bouma *et. al.*, (1980) found that the use of soil survey data (in the estimation of regional evapotranspiration rates) was the most efficient means of providing data for their model compared to other alternatives. The other alternatives ranged from assuming an spatially homogenous soil cover to intensive measurement campaigns (including laboratory analysis) of the soil cover. Efficiency was defined in terms of financial cost, manpower expenditure and accuracy of results.

(b) Moisture transport equation

Under isothermal conditions the transport of moisture through a permeable medium such as a soil is conceived as being essentially analogous to the transport of heat (Marshall

and Holmes, 1979). Thus the general transport equation is similar to that for heat:

$$(7) \quad \frac{d\theta}{dt} = D \frac{d^2\theta}{dz^2}$$

where  $D$  is the soil water diffusivity and  $\theta$  is volumetric moisture content.  $D$  is assumed to be constant in equation (7). In practice, soil water diffusivity varies with water content and the structure and mineralogy of the soil such that;

$$(8) \quad D = K(\theta) \frac{d\theta}{d\psi}$$

where  $K(\theta)$  is the hydraulic conductivity of the soil. The rate of change of the soil water content with respect to the soil matric potential (i.e.  $d\theta/d\psi$ ) describes the characteristic moisture curve for a specific soil (Ward, 1974). The actual form of the curve is dependent on the mineralogy, particle size distribution and structure of the soil and whether the soil is being wetted or dried. (see Fig.3). This type of hysteresis loop is most marked for well structured soils and makes it difficult to uniquely define a value for the soil moisture diffusivity.

Combining equations 7 and 8 gives the generalised expression for the transport of moisture in a heterogeneous material like soil under isothermal conditions;

$$(9) \quad \frac{\partial\theta}{\partial t} = \frac{\partial}{\partial z} \left[ K(\theta) \frac{\partial\psi}{\partial\theta} \cdot \frac{\partial\theta}{\partial z} \right] + \frac{\partial K(\theta)}{\partial z}$$



In the field, isothermal conditions are as rare as steady state conditions. A change in temperature affects soil moisture movement through its influence upon the physical characteristics of the moisture. In the liquid phase, an increase in <sup>temperature</sup> reduces viscous and surface tension forces. In the vapour phase, the vapour pressure of moisture increases substantially with an increase in temperature. In both cases, the overall effect is to induce a flow of water along a temperature gradient from hot to cold regions (Marshall and Holmes, 1979). During daylight hours, the net positive receipt of radiant energy in most locations means that the temperature of the surface is greater than it is at depth. This thermal gradient induces a movement of water from the surface to the deeper, cooler layers. At night the situation is reversed. The result is a diurnal fluctuation of surface soil moisture imposed upon a steadily decreasing moisture content for a drying soil over a period of days (Fig.4)

The generalised equation for soil water movement under non-isothermal conditions is :

$$(10) \quad \frac{\partial \theta}{\partial t} = \frac{\partial}{\partial z} \left[ (K_{w\psi} + K_{v\psi}) \frac{d\psi}{dz} \right] + \frac{\partial}{\partial z} \left[ (K_{wT} + K_{vT}) \frac{dT}{dz} \right]$$

where  $K_{w\psi}$  is the soil water conductivity under a matric potential,  $K_{v\psi}$  is the soil vapour conductivity under a matric potential,  $K_{wT}$  is the soil water conductivity under a thermal gradient and  $K_{vT}$  is soil vapour conductivity under a thermal gradient. Figures 5 (a) and (b) show the magnitudes of the water and vapour conductivities under an hydraulic and a

temperature gradient respectively.  $K_v \psi$  is negligible compared to  $K_w \gamma$  for commonly found values of soil matric potential. In the case of thermally induced flow, vapour transport becomes dominant in dry soils, as shown by Figure 5(a). Although the quantity of moisture transported by this latter mechanism is small compared to that transported by infiltration and percolation processes (which are dominant under saturated conditions), it still an important means of diffusing thermal energy throughout the soil body.

#### (4.2) The Algorithms

Numerous procedures for the evaluation of the components of energy and mass exchanges at the earth's surface can be found in the literature. Due to complexity of these exchanges and fluxes together with the practical constraints of limited data, length of computation, etc., each procedure rests upon many simplifying assumptions. These assumptions depend upon the type of available data (quality and resolution of imagery, scope of ground control data, etc.), the information required (soil moisture, evaportive flux, thermal inertia), and the available analytical tools (image processing techniques, computer capacity, etc.). Although thermal infra-red has many uses (e.g. in thermal pollution studies of urban areas or of the sea, energy conservation, etc.), attention is given here to its use in surveying surface soil moisture and geology.

If the energy flux at the surface of the earth is approximated by a simple cosine function (i.e  $Q=Q_0 \cos \omega t$ ), the solution of the heat diffusion equation (5) is;

$$(11) \quad T(z, t) = T_{av} + A_o \cdot \exp \left[ \left( -\sqrt{\frac{\omega}{2k}} \cdot z \right) \right] \cdot \sin \left( \omega t - \sqrt{\frac{\omega}{2k}} \cdot z \right) \quad \text{PAGE 17}$$

where  $T_{av}$  is the average surface temperature and  $A_o$  is the amplitude of the diurnal surface temperature wave. Thus, at the surface ( $z=0$ );

$$(12) \quad T(t) = T_{av} + A_o \cdot \sin \omega t$$

where  $T \rightarrow T_{av}$  as  $z \rightarrow \infty$ . The amplitude  $A_o$  is dependent on period of cycle ( $2\pi/\omega$ ), the variation in incident radiation ( $Q_o \cdot \cos \omega t$ ) and the thermal characteristics of the medium such that;

$$(13) \quad A_o = \frac{2 Q_o}{\sqrt{\omega} \cdot P}$$

where  $P (= \lambda \rho c)$  is defined as the thermal inertia. If the diurnal temperature wave of an exposed surface is sampled at its extremes (i.e. just before dawn and in the early afternoon), the temperature difference between these two points will approximate to the amplitude of the temperature wave ( $A_o$ ). A knowledge of  $Q_o$  and subsequent use of equation 13 can therefore yield thermal inertia values for the surface. The thermal inertia of a soil body is dependent, in decreasing order of importance, upon its moisture content, its porosity and mineralogy. In the absence of the former two (e.g. in bare rock outcrops in arid regions such as Oman), thermal inertia is indicative of the geology alone (Pohn et. al., 1974).

The Goddard Space Flight Centre in Maryland, U.S.A., produces a data product termed the 'Apparent Thermal Inertia' (ATI) from original thermal infra-red data gathered by the Heat Capacity Mapping Mission Sattelite (HCMM). This data product has 'hopefully many of the attributes of the real thermal inertia' (HCMM Users Guide, 1980).

$$(14) \quad ATI = \frac{NC(1-\alpha)}{\Delta T_R}$$

where N is a scaling factor, C is the correction for the astronomic and temporal variation of sun angle,  $\alpha$  is the albedo of the surface and  $\Delta T_R$  is the radiometric temperature difference for the diurnal cycle. Comparing this to equation 13 indicates that the energy flux at the surface is estimated from albedo measurements and sun angle corrections alone. The use of relative values of temperature (i.e.  $\Delta T$ ) may offset some systematic errors introduced by the radiometer, but errors introduced by topographic slope effects, meteorological factors, moisture fluxes, etc. cannot be assumed to cancel out and all contribute to the final thermal image. More sophisticated approaches have therefore been developed to more accurately interpret thermal infra-red data.

The most common approach to the interpretation of thermal infra-red data has been to develop a sophisticated model based on all the major components of energy exchange at the earth's surface. These include the net longwave and shortwave radiative fluxes ( $E_n$ ), the sensible (H) and latent heat loss (L.E) to the atmosphere (where L is the

latent heat of evaporation for moisture and  $E$  is the net evaporation) and sensible heat loss to the ground ( $G$ ). The first law of thermodynamics requires that;

$$(15) \quad E_n + G + H + L.E = 0$$

Due to the non-linear behaviour of the components of this equation, it must either be solved (for a specific variable) by numerical techniques or, alternatively, linear approximations must be found. These are considered in turn.

#### (4.3). Numerical Models.

Concurrent with the development of high-speed computers has been a growth in the number of numerical techniques for dealing with equations which are not soluble by analytical means. Frequent use <sup>has been</sup> made of explicit finite difference techniques to obtain successive values of surface temperature over specified time periods and for specified boundary conditions (energy fluxes) (e.g. Gillespie and Kahle 1977, Soer 1980, Balick et. al. 1981). In this, the surface layer is divided arbitrarily into a two dimensional mesh, with dimensions of time and depth (Figure 6). Each point on the mesh is given an initial temperature value at time  $t=0$ . The temperature at the next time step ( $t=1$ ) is then computed for each layer ( $z$ ) from the explicit finite difference form of the heat conduction equation:

$$(16) \quad T(t+1, z) = T(t, z) + \lambda (\Delta t / \Delta z^2) [T(t, z+1) - 2T(t, z) + T(t, z-1)]$$

The updated value of surface temperature,  $(T(t+1), 0)$  is then used in the separate evaluation of each component of the energy balance equation to meet the condition that;

$$(15) \quad E_n + G + H + L.E = 0$$

Surface temperature is then iteratively adjusted until convergence is achieved. The process is repeated for the following time steps  $(t+2, t+3, \dots, t+n)$ .

This skeletal outline of the most common numerical models fails to depict the confusing variety of approaches used at a more detailed level. This variety is especially evident when the large number of expressions for the components of equation 15 is considered. An adequate comparison and assessment of these expressions for the purposes of remote sensing is lacking. A general criticism which can be made is that many of them require comprehensive ground information and do not therefore qualify as 'remote sensing' techniques (Watson 1981).

#### The soil heat flux(G)

Complete solution of the heat conduction equation (whether in analytical or finite difference form) requires a large amount of data. This is especially true for a heterogeneous material like soil. The inherent heterogeneity of soil with depth can be approximated by dividing it into a number of sub-layers, each of which is homogeneous with respect

to relevant physical properties. Deardoff (1978) concluded that, in comparison to other models, a twelve layer soil model was the most efficient for calculating the soil heat flux. Although accounting for the variability of soil properties, multi-layered soil models are too data demanding for remote sensing purposes. To side-step the problem of using the heat conduction equation (5), a number of simpler approximations to the soil heat flux has been developed. Many of these link (G) to some other component of the energy balance at the earth's surface (e.g. the net radiative flux, the sensible heat flux etc.). A selection of the methods is given in Table 2.

Sensible and Latent Heat Exchanges with the Atmosphere.

Unlike the transport of heat into the ground, which is dominated by conduction processes, transport mechanisms operating between the surface and the atmosphere are, in general, governed by turbulence. An exception has to be made for the atmospheric layer immediately adjacent to the ground. In this layer (which varies from an order of millimetres to centimetres), laminar flow predominates. Laminar flow is characterised by an orderly and predictable movement of particles with more or less parallel trajectories. The transfer of momentum ( $M$ ), sensible ( $H$ ) and latent heat ( $L.E$ ) through the laminar zone is governed by the respective diffusion equations:

$$(17) \quad M = \rho \nu (\Delta u / \Delta z)$$

$$(18) \quad H = \rho c k_h (\Delta T / \Delta z)$$

$$(19) \quad L.E. = L \cdot \rho \cdot d \cdot (\Delta q / \Delta z)$$

where ( $k_h$ ) is the thermal diffusivity, ( $d$ ) the diffusivity of air particles and ( $\nu$ ) is the kinematic viscosity. Turbulent flow is characterised by violent and random movement of particles superimposed upon an average flow path. Using the analogy of the molecular transfer of sensible and latent heat as defined by equations 17 to 19, turbulent transfers of these quantities can be characterised by substituting the



coefficients ( $K_h$ ) in 18 and ( $d$ ) in 19 by turbulent exchange equivalents. Thus, for sensible and latent heat exchanges in a turbulent atmosphere;

$$(20) \quad H = \rho c K_H (\Delta T / \Delta z)$$

$$(21) \quad L.E. = L \cdot \rho K_W (\Delta q / \Delta z)$$

where  $K_H$  and  $K_W$  are the turbulent exchange coefficients for sensible and latent heat respectively. Unlike their laminar flow counterparts, however,  $K_H$  and  $K_W$  vary widely with differing conditions. The molecular thermal diffusivity ( $k_h$ ) has values ranging from  $0.16 - 0.24 \text{ cm}^2 \text{ s}^{-1}$  whereas  $K_H$  commonly varies over several degrees of magnitude ( $10^2 \text{ cm}^2 \text{ s}^{-1}$  under a temperature inversion to  $10^5 \text{ cm}^2 \text{ s}^{-1}$  for afternoon convective activity) (Oke, 1978). The values of  $K_H$  and  $K_W$  are dependent upon the stability or turbulent regime of the overlying atmosphere which may be characterised by the wind speed and temperature profiles. There are three major regimes, viz. stable, neutral and unstable (Montieth, 1975). The existence of each regime is dependent on the ratio between bouyancy forces (free or natural convection, which is a function of the temperature gradient  $\Delta T / \Delta z$ ) to the mechanical force imparted to the atmosphere by the ground surface (which is a function of wind speed  $U$  and surface roughness). This ratio is given by Richardson's number:

$$(22) \quad R_i = \frac{g}{T} \cdot \frac{\partial T}{\partial z} / \left( \frac{du}{dz} \right)^2$$

For neutral conditions  $Ri$  is unity; for lapse (unstable) conditions  $Ri > 1$ ; and for stable (inversion) conditions  $Ri < 1$ . A wide array of more or less empirical functions based on  $Ri$  have been developed to calculate the sensible and latent heat fluxes within each stability regime. Monin and Obukov (1954), for example, derived the following dimensionless expression for the wind profile from dimensional analysis;

$$(23) \quad \frac{Ri \cdot z}{u_*} \frac{du}{dz} = \phi(Ri)$$

where  $k$  is von Karman's number (0.4),  $u_*$  is the friction velocity of the wind speed profile (the ratio between shear stress and the air density) and  $\phi$  is the turbulent exchange coefficient. There is, however, still no fundamental theory available to predict the functional form of the sensible or latent heat exchange coefficients ( $K_H$  or  $K_w$ ) (Leuning and Attiwell, 1978). They have to be derived experimentally.

### The Radiative flux

The final component of equation 15 is the net radiative flux ( $R_n$ ) at the surface of the earth. This quantity is dependent upon the relative magnitudes of incident solar radiation ( $R_s$ ), the albedo of the surface ( $\alpha$ ), the temperature ( $T_g$ ) and emissivity ( $\epsilon_g$ ) of the surface and the effective temperature ( $T_s$ ) and emissivity ( $\epsilon_s$ ) of the sky hemisphere. These factors are related by the following expression;

$$(24) \quad E_n = E_s (1 - \alpha) + \epsilon_s T_{sky} - E_g T_g^4$$

The albedo of a surface refers to its reflectance integrated over the total solar wavelength spectrum. There are several problems involved in its definition. Radiometers only sample the reflectance of a surface over a limited range of wavelength bands. Furthermore, the reflectance of a surface is not a simple and unique property, but is strongly dependent upon illumination angle, viewing angle and wavelength. Similar problems are encountered to a lesser degree with respect to the emissivity of the surface and the sky. The latter is highly dependent upon the moisture content of the atmosphere. Sellers (1965) presents a number of empirical expressions for the calculation of this quantity. These problems are exacerbated when the topographic surface is non-uniform.

#### (4.4). Analytical Models

Numerical models, although highly accurate in some situations, are costly in terms of the computer facilities they require. Also the expressions they use (e.g. in explicit finite difference or Laplace transform solutions) often have no physical significance. Because of these factors, and partly as a reaction against the inelegance of 'brute force computations' (Price, 1980), several authors have concentrated upon devising more analytical models of the energy flux at the earth's surface for use in thermal infra-red remote sensing (e.g. Watson, 1979; Price, 1977; 1980; Pratt et. al., 1980).

In order to provide an analytical solution of equation 15, linear approximations to the components discussed in the previous section must be found. A common strategy is to assume that the sensible(H) and latent heat (LE) can be approximated by linear expressions of the form;

$$(25) \quad (H + LE) = A + B.T_g$$

where A and B are constants, and  $T_g$  is the ground temperature (Pratt et. al, 1980; Price, 1977). The sensible heat flux is calculated from the following expression;

$$(25) \quad H = d.(T_a - T_g)$$

where  $T_a$  is the air temperature,  $T_g$  is the ground temperature and d is a coefficient which depends on the wind speed, the height of the measuring instruments above the ground and the roughness of the surface. This equation assumes neutral conditions and a constant wind speed over the diurnal period, both of which can lead to notoriously inaccurate results (Businger et. al, 1971). Since heating of the air, in non-advective situations, is controlled by surface temperature, there is normally a phase lag of about two hours between the surface temperature cycle and the air temperature cycle. This physical link may be used to establish the air temperature from the surface temperature;

$$(26) \quad T_a = a.(T_g - T_g') + T_a'$$

where  $D$  is a constant and  $T_g'$  and  $T_a'$  are average diurnal surface and air temperatures respectively. The latent heat flux is treated in a similar manner, that is, evaporation is dependent on the relative humidity difference between the surface and air and surface relative humidity is a function of surface temperature, etc. From these expressions values for the constants  $A$  and  $B$  in equation 24 may be determined which are hopefully unique for a specific location over a range of limited conditions (Pratt et. al., 1980). Schieldge (1878) and Watson (1980) have developed an alternative approach which stresses the aerodynamic element in sensible heat flux from surface to atmosphere (i.e. they do assume neutral conditions). The expressions they derived are based on the Monin-Obukov dimensional analysis of the boundary layer wind profile defined in equation 23. This method calculates the sensible heat flux from wind speed, ground and air temperature measurements at a single height. However, a uniform surface is required, the latent heat flux must be low and the roughness height of the surface has to be carefully specified for reasonably accurate results.

Having established a linearised expression for equation 15, a solution for the surface temperature may be found by equating the cycle of ground temperature with respect to time and depth with a Fourier series equation  $\phi(x, t)$  which describes the characteristic variation of temperature over the diurnal period in terms of its harmonic components. That is, let;

$$(27) \quad T_g - k \frac{\partial T_g}{\partial x} = \phi(x, t)$$

where  $k$  is a constant related to the constants  $A$  and  $B$  of equation 25. From this Pratt et. al. (1980) derived the following expression:

$$(28) \phi(x, t) = \frac{(1 - \alpha_s) S_0 C t}{B} \cdot \sum_{n=0}^{\infty} A_n \cdot \exp(-k\sqrt{n}x) \cos(n\omega t - \epsilon_n - k\sqrt{n}x)$$

where  $S_0$  is the solar constant,  $\alpha_s$  is the shortwave albedo,  $Ct$  is the shortwave radiation atmospheric transmission coefficient,  $A_n$  and  $\epsilon_n$  are the amplitude and phase of the harmonic components of the solar insolation at the surface with fundamental frequency ( $\omega$ ),  $B$  is the constant defined in equation 25 and  $P$  is the ground thermal inertia. With a knowledge of surface temperature at the extreme points of the diurnal temperature wave (i.e. maximum and minimum temperatures), equation 28 can be solved for the thermal inertia  $P$ . Thus, unlike numerical models, which do not explicitly calculate thermal inertia, all the variables in equation 28 have some physical significance. This, together with their speed of calculation, make analytical models attractive in many situations.

#### (4.5) Summary and Discussion

There are commonly two approaches to the modelling of energy flux at the earth's surface, viz. numerical and analytical. Numerical models, although more accurate than their analytical counterparts, demand high speed computer facilities and the expressions used in the computation often

have little or no real physical significance. Analytical models, however, only give reasonable results for a limited range of conditions which are defined by the assumptions made in arriving at the model. Whether one employs an analytical or a numerical model, therefore, is dependent on the situation (i.e., the information required and the accuracy needed).

Within the context of this paper, the most common uses of thermal infra-red imagery involve the remote sensing of thermal inertia for geological surveying and of soil moisture in hydrology, agriculture, etc. In the case of the former (thermal inertia mapping in geology), it would appear that the use of analytical techniques is more efficient for several reasons. From a theoretical consideration of the components which contribute to the thermal inertia of a soil (e.g. by using the techniques of De Vries (1963)), it can be shown that its value depends much more upon soil moisture content and porosity than upon the mineralogical and textural properties of the soil. Textural properties of soils (i.e. sand, silt, clay) only affect thermal inertia indirectly through their effect upon soil moisture (Pratt and Ellyet, 1978). Even in exceptionally arid zones, the top 10 cm of soil is unlikely ever to be completely dry, especially in fine textured soils. It is therefore difficult to isolate an absolute quantitative value of thermal inertia from thermal infra-red imagery alone. Thermal inertia mapping can only be based on relative values. In this context, it provides a useful qualitative addition for reconnaissance geological surveying through the identification of thermal anomalies (Pohn et. al.

1974; Pohn 1976). Direct identification of geological materials is not possible. Hence, use of high powered numerical techniques are not justified in this situation. Since, however, soil moisture content is so crucial in the thermal behaviour of a soil, together with its role in determining the relative magnitudes of sensible and latent heat, numerical techniques may be used quite successfully in determining its absolute value (Soer, 1980; Elkington 1979).

Finally, it must be pointed out that the distinction between numerical and analytical techniques is one of degree rather than of type. The most efficient means of solving the analytically derived equation 28 for thermal inertia  $P$ , for example, is to use an iterative technique. Some authors have found that the best results come from a compromise between the two approaches. The analytical Fourier model (based on equation 28) has been combined with a numerical iterative technique by both Price (1980) and Hechinger et. al., (1982), thus reconciling the simplicity and rapidity of analytical models with the accuracy of numerical models.



### (5). The Problem of Vegetation

Up to this point all surfaces have been assumed to be free of vegetation. The introduction of a vegetative cover introduces several complications. Those involving the spectral reflectance of the surface are discussed in a complementary paper to this one (Coyle, 1982a). Concentration is given here to the effect of vegetation upon the energy fluxes of a surface with reference to thermal infra-red remote sensing.

The interactions between soil water content, evaporation, transpiration, radiation and vegetation have been intensively researched over many years. The most active area for research has been in establishing the link between soil moisture, vegetation and the evaporative flux. The earliest formulations estimated actual evapotranspiration as a fraction of potential evapotranspiration as defined by Penman (1948) and later expanded, adapted and extended beyond the original constraints of non-limiting water supply by many authors (see Sellars 1965; Montieth 1975). When this fraction fell below unity, evapotranspiration became limited by soil properties rather than by energy input. In the absence of a water table, the moisture content of soils normally lies between field capacity and wilting point (Sellars, 1965). Although they are vaguely defined terms, field capacity and wilting point are useful empiricisms (Ward, 1975). The actual evapotranspiration from a vegetated surface is therefore determined by the position of the soil moisture content relative to field capacity and wilting point (Van Bavel and Hillel, 1976). In

this version of the process, the vegetation plays a passive role. The interactions between the soil, vegetation and atmosphere are more subtle than this however. Evapotranspiration rates may drop, for example, not as a result of limiting moisture but because of plant closure of stomata due to high evaporative demands (Rutter, 1975). More theoretical and generalised models have therefore been developed to account for the complicating effect of vegetation.

The concept of the Soil-Plant-Atmosphere Continuum (SPAC) has formed the basis of many evaporative models of vegetation. These are based on electrical analogues of water movement from the soil to the atmosphere (Figure 7). Moisture movement is governed by the balance of energy potential differences (between soil-root, root-stem-leaf and leaf-atmosphere systems) and the corresponding resistances (which may act in parallel or in series).

SPAC models have varying degrees of complexity. Some may divide the root zone of the soil into several layers and assume that the plant atmosphere system can be represented by a simplified mono-layer evaporative model (e.g. Deardoff, 1978; Balick et. al. 1981). Alternatively, the vegetation canopy may <sup>be</sup> modelled in detail whilst assuming a continuously wet soil or one which is uniformly dry with depth (e.g. Smith et. al. 1981). Combined layered canopy and layered soil models are rare, perhaps because of the large volume of data required by such complex models (Federer, 1979).

There are three major problems involved in the use of SPAC models. Firstly, the complex nature of moisture flow through the SPAC system means that models become rapidly overloaded with parameters designed to characterise the flows, resistances and storage units within the system. (A parameter is a quantity characterising a system which remains constant with time (Clarke, (1973)). One of the simplest and earliest expressions describing the soil-root system is;

$$(29) \quad Q_w = \frac{\psi_{rs} - \psi_{rx}}{R_r}$$

where  $Q_w$  is the rate of flow of water ( $\text{cm}^3 \text{s}^{-1}$ ),  $\psi_{rs}$  is the water potential of the root surface (bar),  $\psi_{rx}$  is the water potential of the root xylem (bar) and  $R_r$  is the resistance of the root system to water flow. In this equation, simplifications include the assumptions of steady state flow conditions (which rarely occur) and a constant value for the parameter  $R_r$  for all transpiration values (which never occurs). Thus a large volume of literature has built up describing ways of accounting for the complexity inherent in the system (see Molz, 1981 for a review). The number of parameters used in the more complex models has increased in a like manner.

The second problem occurs when an attempt is made to obtain values for the parameters of a SPAC model. Most of these parameters are treated in an ambiguous way. In many instances, they form part of a complicated mathematical model. This model is usually calibrated using a required set of field

data (soil moisture content, transpiration rates, etc.). The values of the parameters of the model (e.g. root density, root permeability, air-leaf resistances, etc.) are often chosen by trial and error to make the results of the model fit the data. This is called calibration. If the model can be made to fit the data reasonably well, it is considered to be successful. Ideally, independent testing of the parameters (i.e. independent of the model) are needed. These parameters are however often too ill-defined or too numerous for adequate measurement. Although some authors have attempted independent testing of parameters (e.g. Herkelrath, 1977), most use some form of calibration procedure (e.g. Nimah and Hanks, 1973; Walley and Hussein, 1982) for practical reasons. Finally, the third problem, which is related to the previous two, is that SPAC models generally have an extremely high demand for data. This makes many of them quite useless in a field situation (Ziemar, 1979).

To circumvent the problems associated with these mechanistic models, more empirical equations have been used in order to make use of data which can be obtained at reasonable expense. An example of this approach is the stress degree day (SDD) model (Idso et. al. 1977).

In western agriculture the main determinants of yield are temperature and moisture (Curtis, 1978). When soil moisture is limiting to transpiration, or when high potential evapotranspiration conditions exist, plants tend to close their stomata (Rutter, 1975). The resultant increase in the sensible temperature due to decreased evapotranspiration can

be detected by thermal infra-red remote sensors. Thus, the temperature difference between the crop canopy and the air may be used as an indicator of moisture stress in plant canopies. The concept of the stress degree day has been used alongside remotely sensed crop temperature data in the expression;

$$(30) \quad Y = \alpha - \beta \cdot \sum_{i=b}^e SDD_i$$

where SDD<sub>i</sub> is the mid-afternoon (1400 hrs) value of leaf/air temperature difference on day *i*, *b* is the day on which summation begins, *e* is the day on which summation ends and  $\alpha, \beta$  are empirically determined from a least squares regression technique. The best time over which the summation can be made is indicated by changes in the albedo of the crop. These changes occur with the first appearance of the awns (*b*) and at the time when the head produces no more dry matter (*e*). The SDD approach is geographically limited for any pair of  $\alpha$  and  $\beta$  values. Its flexibility may be extended by subtracting the number of days when average daily temperature falls below the level at <sup>which</sup> physiological activity ceases (Idso et. al, 1980). It is more seriously limited however to large field situations common in the wheatlands of the U.S.A. It is more difficult to apply it to small field areas more prevalent in Europe using existing radiometers (Curtis, 1978).

(6). General Discussion

Remote sensing from airborne and space platforms has several important advantages over alternative means of resource evaluation which are based on interpolation between point samples. The ability of remote sensing systems to make quick and frequent inventories of earth resources over large areas is their most attractive feature. These inventories fall into two categories (Hardy, 1980):

(a). The surveying of relatively static earth surface features such as lithology, soil type and topography.

(b). The survey and subsequent monitoring of more dynamic phenomena such as weather systems, soil moisture or vegetation.

Many properties of the earth's surface (such as vegetative cover) may be arbitrarily placed in either category. Soil moisture content, however, is firmly embedded in the latter group of highly dynamic phenomena. Although an initial survey may be able to determine how much moisture a soil can hold between field capacity and wilting point, its soil moisture status at any point in time can only be ascertained through frequent monitoring.

The decision to use remotely sensed data as an alternative to regional estimates of soil moisture from precipitation and potential evaporation data is an economic one (Hardy, 1980). However, the more technological problem of devising a remote

sensing system that works has still to be solved. As yet there is no fully operational method for calculating soil moisture over a large area from remotely sensed data although there are several candidates. With this in mind, the physical principles of remote sensing in the visible and reflective waveband have been reviewed above.

In order to depict the spatial variations of soil moisture, remotely sensed data are organised into resolution cells. These represent the smallest area in a scene which can be considered as a unit. The dimensions of a resolution cell define the smallest angular or linear separation which can occur between two distinct points in, for example, a Landsat image. The value attributed to a cell is the aggregated response of its constituents. The problem then arises as to the physical meaning of this aggregated response. The discrimination between two objects in a Landsat image, for example, is based on the difference between their 'spectral signatures'. The spectral signature attributed to each resolution cell is made up of the reflectance properties of each of its constituents. Because of this, the spectral signature of a heterogeneous ground area may not be representative of any of its constituents.

For thermal infra-red and passive microwave remote sensing, a similar problem is encountered with respect to the meaning of surface temperature. For a truly homogeneous and flat ground surface at thermal equilibrium, the surface temperature is well defined, if not easily measured (Becker, 1980). The surface temperature of an undulating and

heterogeneous<sup>a</sup> surface with a vegetation canopy is much more ambiguous in meaning. Each element within the canopy (stems, leaves and ground surface) contributes to the radiative flux and these contributions vary over time and space. Often some kind of weighting system is used. Smith et. al. (1981), for example, weighted the radiometric temperature of the lowest (of three) layers of a forest canopy most heavily. This ambiguity makes 'ground truth' measurement of surface temperature difficult. This point can be generalised to all remote sensing systems. That is, to enable a check to be made on the accuracy of remotely sensed data, the ground data collection must be organised to take into account the size of the resolution cell involved and its aggregating properties (Hardy, 1980b).

Because of their nature, remote sensing techniques are most sensitive in upper few centimetres of the soil. The extent of penetration into the profile varies with the method used. The visible albedo, for example, is only related to the soil moisture content of a very thin surface layer (less than 0.2 cm. thick) (Idso et. al. 1974). Remote sensing of soil moisture at thermal infra-red wavelengths relies upon the fact that surface temperature (however defined) is an integral response to the energy fluxes between the soil and the atmosphere. It is therefore influenced by the integrated moisture value over the depth of soil which is taking part in these exchanges and it is this 'active layer' which is of most interest to a climatologist or an agriculturalist. Thermal infra-red remote sensing therefore possesses an important advantage in this instance.



A variety of techniques have been developed to exploit remotely sensed thermal infra-red data. These tend to be based largely on a physical - mathematical type of modelling in contrast to the more empirical techniques common to remote sensing in the visible and reflective infra-red wavelengths. The interpretation of Landsat MSS data, for example, rests on the establishment of useful correlations between earth surface features and their 'spectral signatures'. Few surfaces however have unique thermal infra-red signatures (Price, 1980). The reason for the inconsistent thermal behaviour of most surfaces lies in the fact that a 'thermal signature' is not a simple function of surface type and viewing geometry alone. It is, rather, the product of a variety of physical processes (evaporation, radiation, conduction etc.). The meaning of surface temperature therefore remains ambiguous unless these processes are accounted for. Thus the physical - mathematical modelling approach dissects in detail the energy interactions at the earth's surface to arrive at its resultant thermal behaviour.

Thermal inertia mapping can only hope to give a qualitative guide to the geology of an area (Pratt and Ellyet, 1980). In this context it can be a valuable aid when used in conjunction with other sources of information such as existing geological maps and Landsat images (Pohn et. al. 1974; Pohn, 1976). In geological mapping, high powered numerical models such as those developed by Kahle (1977) do not seem as efficient as the more approximate, analytical techniques (Pratt et. al., 1980; Price, 1977) given the inherent limitations of thermal inertia values.

The complexity of numerical models designed to extract soil moisture from remotely sensed thermal infra-red data is potentially great. The present understanding of the physical principles and phenomena relating to soil water flux along the soil plant atmosphere continuum can incorporate many of the dimensions involved (e.g., hysteresis, non-homogeneity, and anisotropy in time and space). In practice, however, the scale of measurement required to meet the data demands of these models is highly prohibitive to their use. A compromise must be reached in which the required accuracy of soil moisture/temperature information specifies which approach or model is the most suitable under the circumstances. Even crude estimates of soil moisture over a large area are of value to disciplines such as hydrology, agriculture and meteorology (Cihlar, 1977).

#### ACKNOWLEDGEMENT

The author is very grateful to Dr J Hogg, his Supervisor, for his advice and help throughout the period of research.

## REFERENCES

PAGE 41

- Baldocchi D.D. Shashi V.B. Rosenberg N.J.  
1981  
Seasonal and Diurnal Variation in the CO<sub>2</sub> Flux and CO<sub>2</sub>-Water Flux Ratio of Alfalfa  
Agricultural Meteorology Vol. 23 pp 231-244
- Balick L.K. Scoggins R.K. Link L.E.  
1981  
Inclusion of a Simple Vegetation Layer in Terrain Temperature Models for Thermal IR Signature Prediction  
IEEE Transactions on Geoscience and Remote Sensing Vol. GE-19 no.3 pp 143-152
- Becker F.  
1980  
Thermal Infra-red Remote Sensing Principles and Applications  
in "Remote Sensing Applications in Agriculture and Hydrology" edited by G. Frayse 1980.
- Bell K.R. Blanchard B.J. Schmugge T.J. Witzak M.W.  
1980  
Analysis of Surface Moisture Variations within Large Field Sites  
Water Resources Research Vol. 16 no.4 pgs 796-810
- Bouma J. De Laat P.J.M. Awater R. Van Beesen H.C. Van Holst A.F. Van de Nes Th. J.  
1980  
Use of Soil Survey Data in a Model for Simulating Soil Moisture Regimes.  
(Proceedings) Soil Science Society of America. Vol. 44 no.4 pgs 808-814.
- Brakke T.W. Verma S.B. Rosenberg N.J.  
1978  
Local and Regional Components of Sensible Heat Advection.  
Journal of Applied Meteorology ; Vol.17 pp 955-963
- Bresler E. Bielorai H. Laufer A.  
1979  
Field Test of Solution Flow Models in a Heterogenous Irrigated Cropped Soil  
Water Resources Research Vol.15 pp 645-652
- Brown K.W.  
1974  
Calculations of Evapotranspiration from Crop Surface Temperatures  
Agricultural Meteorology Vol. 14 pgs 199-209
- Buettner K.J.K. Kern C.D.  
1965  
The Determination of Infrared Emissivities of Terrestrial Surfaces.  
Journal of Geophysical Research Vol.70 no.6 pp 1329-1337
- Butler B.E.  
1980  
Soil Classification for Soil Survey  
Clarendon Press, Oxford
- Byrne G.F. Begg J.E. Fleming P.M. Dunin F.X.  
1979  
Remotely Sensed Land Cover Temperature and Soil Water Status - A Brief Review.  
Remote Sensing of Environment Vol.8 pp 291-305

Cihlar J. McQuillan A.K.

1977

Applications of Sattelite Thermal Infrared Measurements to Earth's Resources Studies

Presented at the Remote Sensing Science and Technology Symposium , Ottawa ,  
21-23 Feb. 1977

Clarke R.T.

1973

A Review of some Mathematical Models used in Hydrology - with observations on their calibration and use.

Journal of Hydrology Vol. 19 pp 1-20

Coleman G.

1979

Pasture-Wheat Temperature Differences : Indicator of Relative Soil Moisture Differences.

Machine Processing of Remotely Sensed Data Symposium. I.E.E.E. pp 224-231

Dyer A.J.

1967

The Turbulent Transport of Heat and Water Vapour in an Unstable Atmosphere.

Quarterly Journal of the Royal Meteorological Society Vol. 93 pp 501-508.

Elkington M.D.

1979

An approach to characterising the water content of soils by thermalinfrared remote sensing

Working Paper no.262

Federer C.A.

1975

Evapotranspiration

Reviews of Geophysics and Space Physics Vol.13 no.3 pp 442-445

Frayse G.

1980

Remote Sensing Applications in Agriculture and Hydrology

A.A. Balkema , Rotterdam.

Gillespie A.R. Kahle A.B.

1977

Construction and Interpretation of a Digital Thermal Inertia Image

Photogrammetric Engineering and Remote Sensing Vol.43 no.8 pp 983-1000

Green F.H.W. Harding R.J.

1979

The Effects of Altitude on Soil Temperature

Meteorological Magazine Vol. 108 pgs 81-91

Harding R.J.

1979

Radiation in the British Uplands.

Journal of Applied Ecology Vol. 16 pgs 161-170.

Harrrod T.R

1978

Soil Survey Record no. 47

- Rothamsted Experimental Station, Harpenden, Herts, England.
- Hatfield J.L. Reginato R.J. Jackson R.D. Idso S.B. Pinter P.J.  
1978  
Remote Sensing of Surface Temperature for Soil Moisture, Evapotranspiration and Yield Estimation.  
Fifth Canadian Symposium on Remote Sensing , Victoria. pp 460-466
- Herklerath W.N. Miller E.E Gardner W.R.  
1977  
Water Uptake by Plants 2; The Root Contact Model  
Soil Science Society of America. (Proceedings). Vol.41 pp.1039-1043
- Hevley J.D. Hewlett J.D. Douglass J.E.  
1972  
Predicting Soil Moisture in the Southern Appalachians  
Proceedings: Soil Science Society of America Vol. 36 pgs 954-
- Hielman J.L. Moore D.G.  
1981  
Heat Capacity Mapping Mission Data  
Remote Sensing of the Environment Vol. 11 no.1 pgs 73-79.
- Idso S.B. Jackson R.J. Reginato R.J. Kindall B.A. Nakayama F.S.  
1975  
The Dependence of Bare Soil Albedo on Soil Water Content  
Journal of Applied Meteorology Vol.14 pgs 109-113
- Idso S.B. Reginato R.J. Jackson R.D.  
1979  
Calculation of Evaporation during the Three Stages of Soil Drying  
Water Resources Research Vol. 15 pp 487-488
- Idso S.B. Hatfield J.L. Jackson R.D. Reginato R.J.  
1979  
Grain Yield Prediction: Extending the Stress Degree Day Approach to Accomodate Climatic Variability  
Remote Sensing of Environment Vol. 8 pp 267-272
- Jackson R.D. Reginato R.J. Idso S.B.  
1977  
Wheat canopy temperature : A practical tool for evaluating water requirements.  
Water Resources Research Vol. 13 no.3, pgs 651-656
- Kahle A.B. Gillespie A.R. Goetz A.F.H. Addington J.  
1975  
Thermal Inertia Mapping  
Proceedings Tenth Symposium on R.S.E. pgs 985-994
- Kaimal J.C Wyngaard J.C. Haugen D.A.  
1976  
Turbulence Structure in the Convective Boundary Layer  
Journal of the Atmospheric Sciences Vol.33 pp. 2152-2169
- Leuning R. Attiwell P.M.  
1978  
Mass, Heat and Momentum Exchange between a Mature Eucalytus Forest and the Atmosphere.

Agricultural Meteorology Vol.19 pp. 215-241

Luxmoore R.J. Sharma M.L.

1980

Runoff Responses to Soil Heterogeneity : Experimental and Simulation Results from Two Contrasting Watersheds.

Water Resources Research Vol. 16 no.4 pgs 675-684

Luxmoore R.J. Stolzy J.L. Holdeman J.T.

1981

Sensitivity of a Soil-Plant-Atmosphere Model to Changes in Air Temperature , Dew Point Temperature, and Solar Radiation

Agricultural Meteorology Vol. 23 pp 115-129

Marshall T.J. Holmes J.W.

1979

Soil Physics

Cambridge University Press, Cambridge.

Mckim H.L. Walsh J.E. Arion D.M.

1980

Review of Techniques for measuring Soil Moisture in Situ

United States Army Corps of Engineers Special Report 80-37

Molz F.J.

1981

Models of Water Transport in the Soil Plant System

Water Resources Research Vol.17 no.5 pp 1245-1260

Monteith J.L. (ed.)

1975

Vegetation and the Atmosphere 2 Volumes: Vol.1 Principles ; Vol.2 Case Studies

Academic Press , London. 278 pages.

Morrison D.B. Scherer D.J.

1977

Machine Processing of Remotely Sensed Data Symposium.

Laboratory for Applications of Remote Sensing (LARS) Purdue University , W. Lafayette U.S.A.

Motha R.P. Verma S.B. Rosenberg N.J.

1979

Exchange Coefficients under Sensible Heat Advection Determined by Eddy Correlation

Agricultural Meteorology Vol.20 pp 273-280

Nimah M.N. Hanks R.J.

1973

Model for Estimating Soil, Water , Plant and Atmospheric Inter-relations.

Soil Science Society of America (Proceedings) Vol. 37 pp 522-531

Oke T.R.

1978

Boundary Layer Climates

Methuen and Company Ltd. London

Parton W.J. Logan J.A.

1981

A Model for Diurnal Variation in Soil and Air Temperature  
Agricultural Meteorology Vol. 23 pp 205-216

Paulson C.A.  
 1970

The Mathematical Representation of Wind Speed and Temperature Profiles in the  
 Unstable Atmospheric Surface Layer.  
Journal of Applied Meteorology Vol.9 pp. 857-861

Pohn H.A. Offield T.W. Watson K.  
 1974

Thermal Inertia Mapping from Sattellites- Discrimination of Geologic Units in  
 Oman.  
Journal of Research of the U.S. Geological Survey. Vol.2 no.2 pp 147-158

Pohn H.A.  
 1976

A Comprison of Landsat Images and Nimbus Thermal Inertia Mapping of Oman  
Journal of Research of the U.S. Geological Survey Vol.4 pp 661-665

Pratt D.A. Ellyett C.D.  
 1979

The Thermal Inertia Approach to Mapping of Soil Moisture and Geology  
Remote Sensing of Environment Vol.8 pp 151-168

Price J.C.  
 1981

The Contribution of Thermal Data in Landsat Multispectral Classification  
Photogrammetric Engineering and Remote Sensing Vol. 47 no.2 pp 229-236

Price J.C.  
 1979

Surface temperature variations as measured by the Heat Capacity Mapping Mission  
Int. Symp. on R.S.E. Part 2 pgs 765-770

Price J.C.  
 1980

The potential of remotely sensed thermal infrared data to infer surface soil  
 moisture and evaporation  
Water Resources Research Vol. 16 no. 4 pgs 787-795

Ragan R.M.  
 1978

Utilisation of remote sensing observations in hydrologic models  
Proceedings of the 11th Symp. on R.S.E. (Ann Arbor , Michigan) pgs 87-95

Reginato R.J. Idso S.B. Vedder J.F. Jackson R.D. Blanchard M.B. Goettelman  
 R.  
 1976

Soil water content and evaporation determined by thermal parameters obtained  
 from ground based and remote measurements  
Journal of Geophysical Research Vol. 81 no.9 pgs 1617-1620

Rosema A.  
 1975

Heat Capacity Mapping; Is It Feasible?  
Proceedings of the 10th. Symp. on R.S.E. (Ann Arbor Michigan) pgs 571-582

Rowan L.C. Lathram E.H.  
1980

Mineral Exploration

Chapter 17 in "Remote Sensing in Geology" edited by B.S Siegal and A.R. Gillespie

Salmonsens V.V. Rango A.  
1980

Water Resources

Chapter 18 in "Remote Sensing in Geology" edited by B.S. Siegal and A.R. Gillespie.

Saxton K.E.  
1975

Sensitivity Analyses of the Combination Evapotranspiration Equation.  
Agricultural Meteorology ; Vol. 15 pp 343-353

Schildge J.P.  
1978

On Estimating the Sensible Heat Flux over Land  
Agricultural Meteorology ; Vol 19 pp 315-328

Schmugge T.J. Jackson T.J. Mckim H.L.  
1980

Survey of methods for soil moisture determination  
Water Resources Research Vol. 16 no.6 pgs 961-979

Schnieder S.R. McGinnis D.F. Pritchard J.A.  
1979

Use of Sattelite Infrared Data for Geomorphology Studies  
Remote Sensing of Environment Vol.8 pp pp 313-330

Sellers W.D.  
1965

Physical Climatology , University of Chicago Press ;  
University of Chicago Press ,Chicago and London.

Siegal B.S. A.R. Gillespie  
1980

Remote Sensing in Geology  
John Wiley and Sons New York. 702 pages.

Smith J.A. Ranson K.J Nguyen D. Balick K. Link L.E. Fritschen L. Hutchison B.  
1981

Thermal Vegetation Canopy Model Studies  
Remote Sensing of Environment Vol.11 pp 311-326

Smith W.L.(ed.)  
1977

Remote Sensing Application for Mineral Exploration  
John Wiley and Sons , New York.

Taylor S.E.  
1979

Measured Emissivity of Soils in the Southwest United States  
Remote Sensing of Environment Vol.8 pp 359-364



Van Bavel C.H.M. Hillel D.I.  
1976

Calculating Potential and Actual Evapotranspiration from a Bare Soil Surface  
by Simulation of Concurrent Flow of Water and Heat  
Agricultural Meteorology Vol. 17 pp 453-476

Walley W.J. Hussein D.E.D.A.  
1982

Development and Testing of a General Purpose Soil-Moisture-Plant Model  
Hydrological Sciences Journal Vol. 27. no.1 pp. 1-17

Watson K.  
1980

Direct Computation of the Sensible Heat Flux  
Geophysical Research Letters Vol.7 pp.616-618

Watson K.  
1974

Geologic applications of thermal infrared images  
Annals of the Inst. of Electrical and Electronic Engineers Inc. pgs 128-137

Watson K. Hummer-Miller S.  
1981

A Simple Algorithm to Estimate the Effective Regional Atmospheric Parameters  
for Thermal Inertia Mapping.  
Remote Sensing of Environment Vol.11 pp. 455-462.

Ziemer R.R.  
1979

Evaporation and Transpiration  
Review of Geophysics and Space Physics Vol. 17 pp. 1175-1186

ASTRONOMICAL -TEMPORAL	ATMOSPHERIC	TOPOGRAPHIC	SURFACE	SUBSURFACE SOIL
Latitude	Temperature	Slope	Albedo	Thermal Conductivity
Time of Year	Wind Speed	Aspect	Emissivity	Thermal Capacity
Time of Day	Cloud Cover	Altitude	Vegetation	Composition (Moisture, bulk density et
			Roughness	

Environmental Variables effecting Surface Temperature

TABLE 1

1. Multiple (12) soil Payers	Finite difference solution of diffusion equation $G = -\lambda dT/dz$	Balick et al. (1981)
2. Insulated Surface	$G = 0$	Gates et al. (1971)
3. Steady state (averaged over diurnal period)	$\int G dt = 0$ 24 hours	Price (1980)
4. Sensible heat dependence	$G = f^H(H)$	
5. Rnet dependence	$G = f^H(R_{net})$	Deardoff (1978)
6. Dependence on sum of fluxes to the atmosphere	$G = f^H(R_{net}, H, L.E.)$	
7. Surface temperature ( $T_g$ ) dependence	$G = f^H(T_g)$	Elkington (1979)
8. Empirical curve fitting e.g. Fourier analysis sine/exponential curve approximations		Parton et al. (1981)

TABLE .2

Various Methods of Calculating : Heat Flux (G)

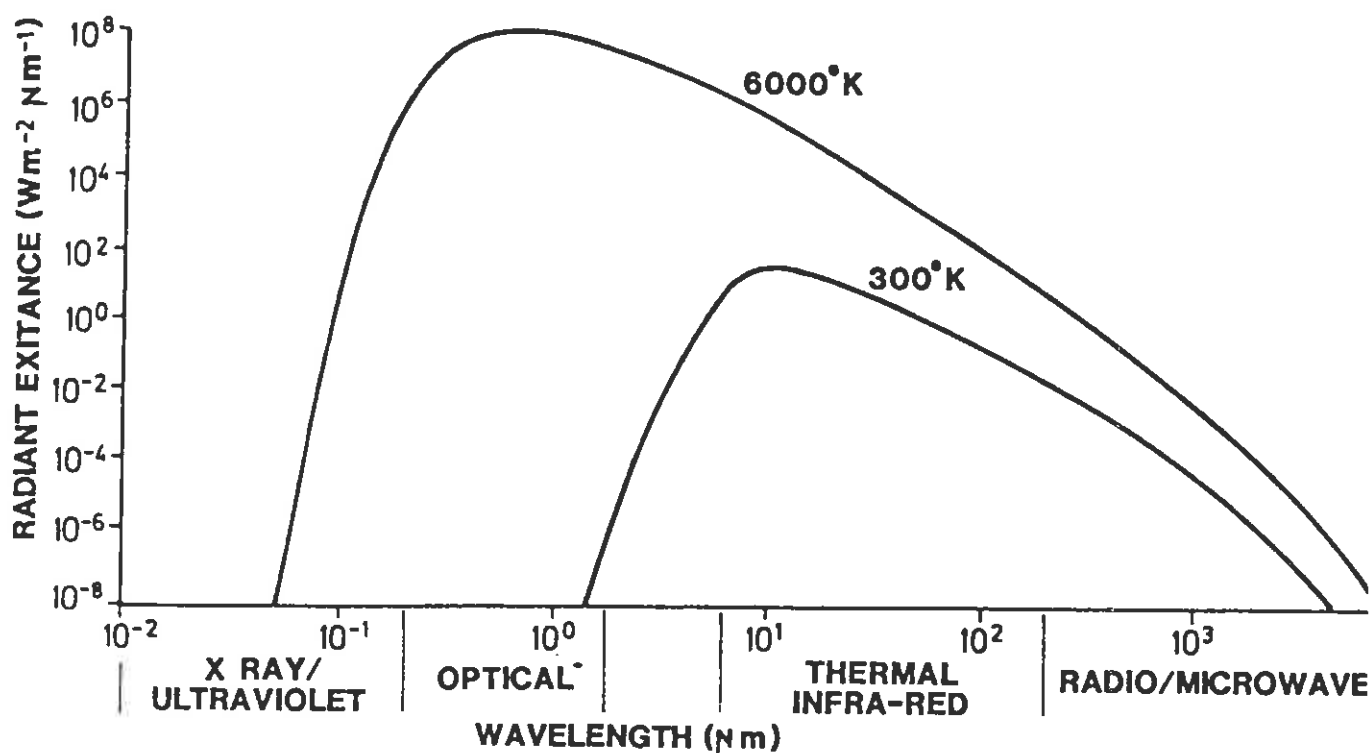


FIG. 1. "BLACK-BODY" RADIATION CURVES

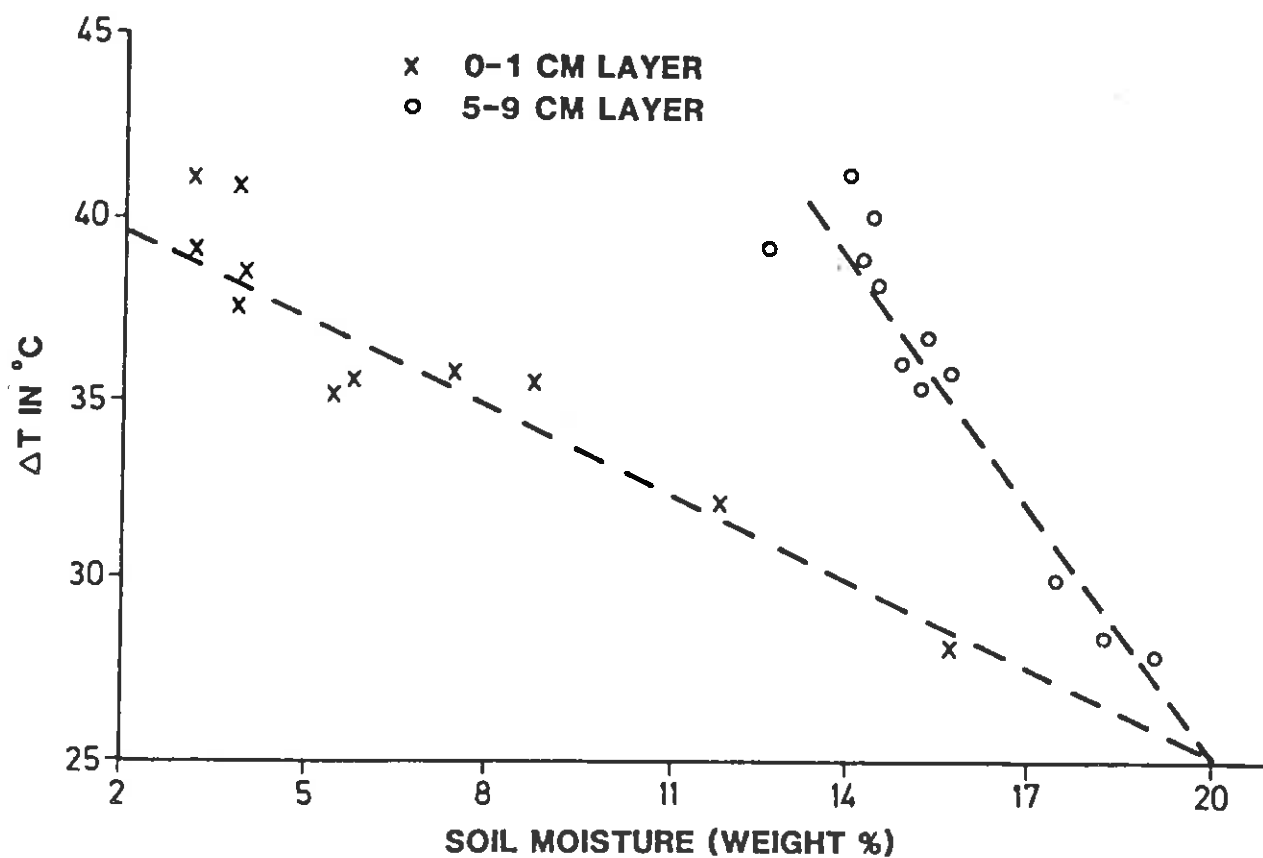


FIG.2. DIURNAL TEMPERATURE VARIATION VS. SOIL MOISTURE

(REPRODUCED FROM ELKINGTON, 1979, AFTER JACKSON, 1973)

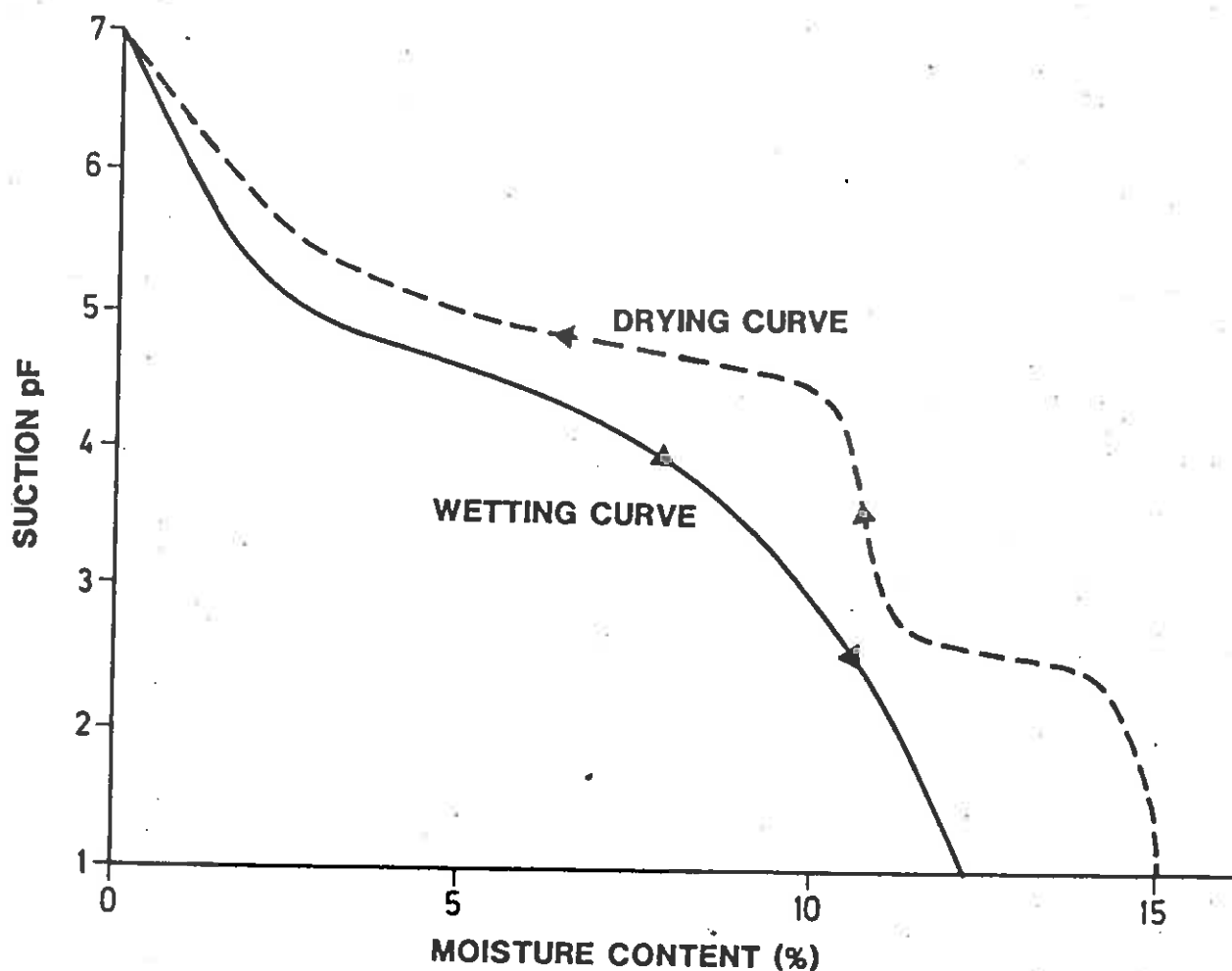


FIG. 3. HYSTERESIS LOOP FOR SILTY CLAY

(AFTER WARD, 1975)

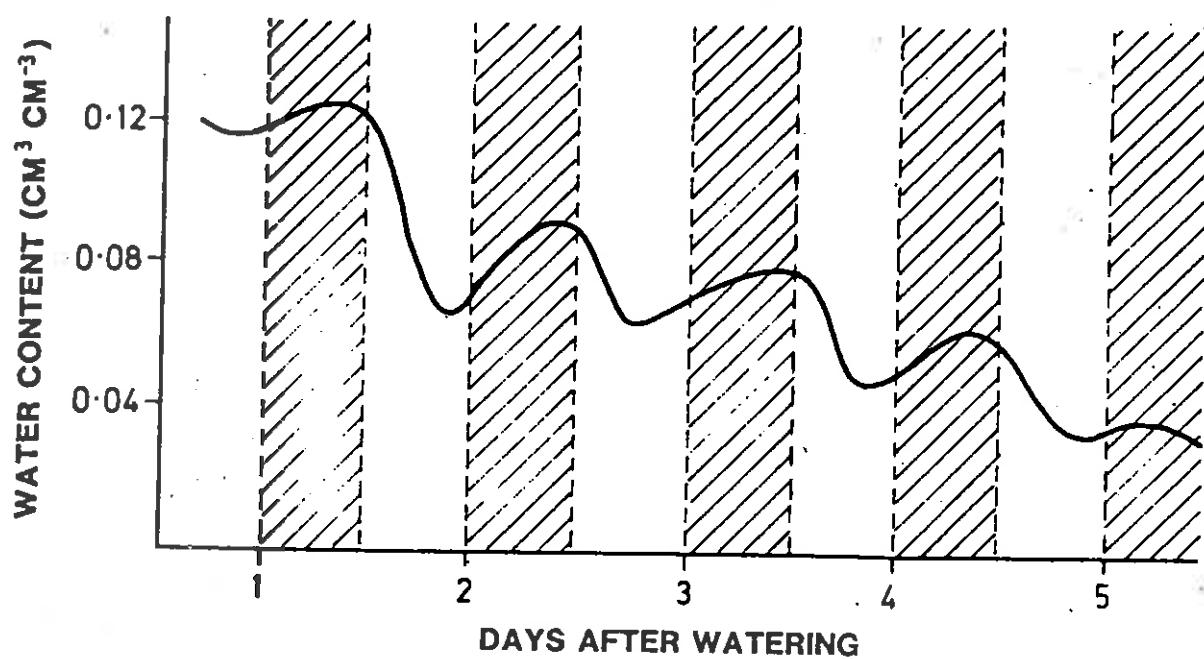


FIG. 4. FLUCTUATIONS IN WATER CONTENT OF SOIL CAUSED DIURNAL TEMPERATURE CYCLE (IN 0-3 CM LAYER) NIGHT PERIODS ARE SHOWN BY SHADING

(AFTER ROSE, 1968)

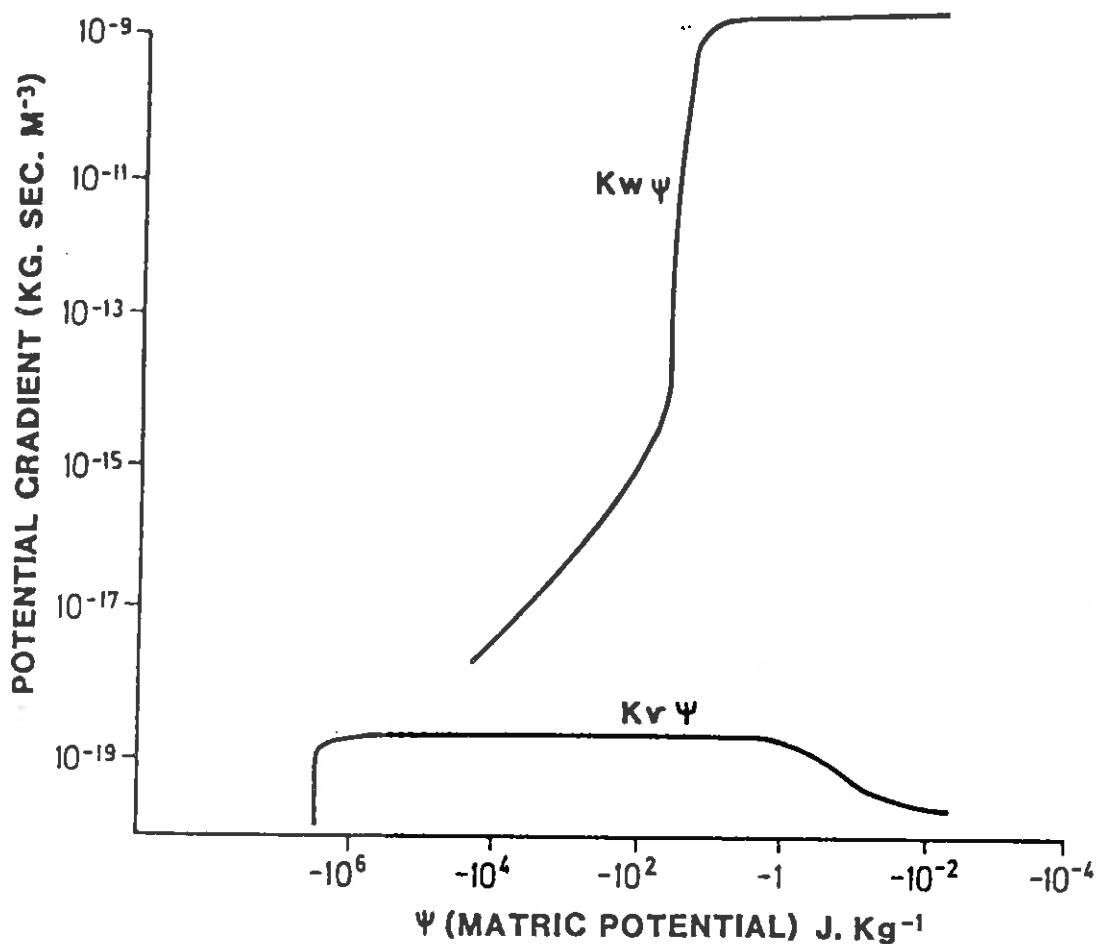


FIG. 5(a). THE RELATIONSHIP BETWEEN MATRIC POTENTIAL OF SOIL, POTENTIAL GRADIENTS AND WATER AND VAPOUR CONDUCTIVITIES ( $K_w$ ,  $K_v$ )

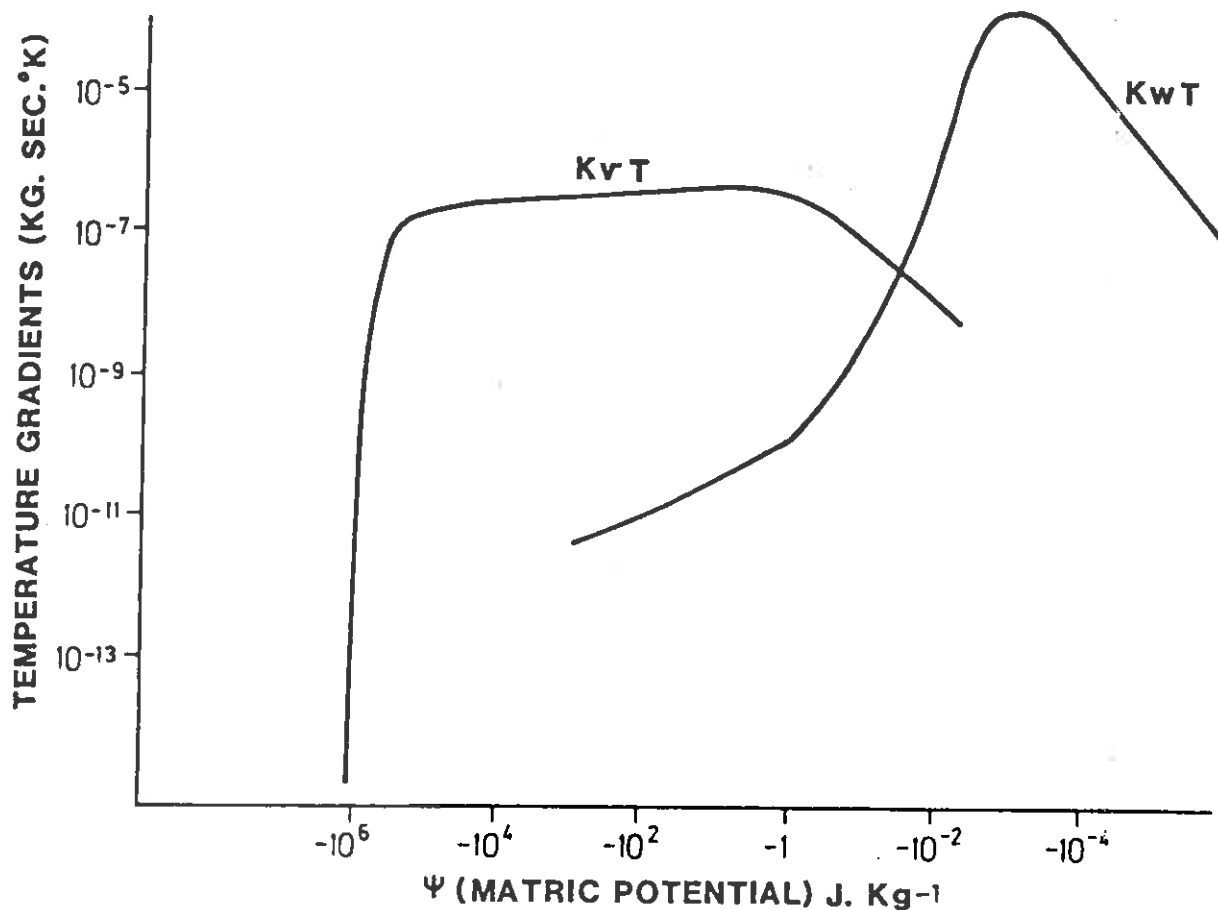


FIG. 5(b) THE RELATIONSHIP BETWEEN MATRIC POTENTIAL OF SOIL, TEMPERATURE GRADIENTS AND WATER AND VAPOUR CONDUCTIVITIES (AFTER ROSEMA. 1951)

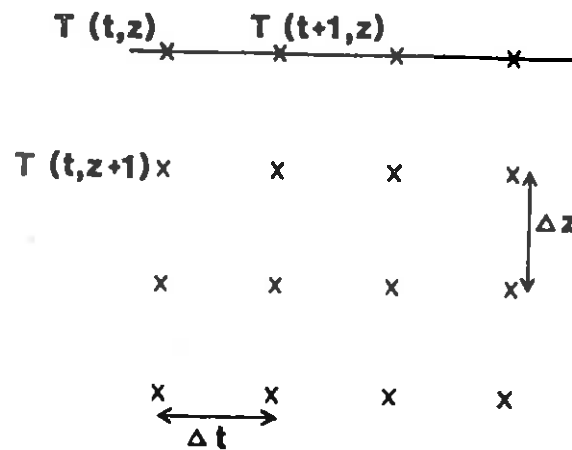


FIG. 6. TWO DIMENSIONAL MESH USED IN THE SOLUTION OF EXPLICIT FINITE DIFFERENCE HEAT EQUATION. (2.16).  
Z IS DEPTH, t IS TIME, T IS TEMPERATURE.

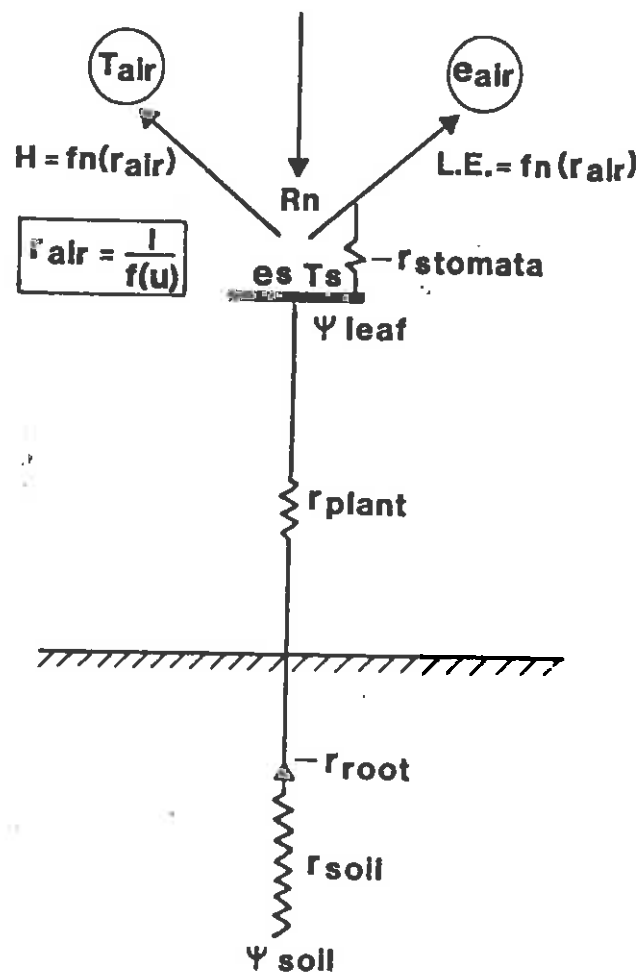


FIG.7. SIMPLIFIED DIAGRAM OF A SPAC MODEL.  
r IS RESISTANCE, u IS WIND, T IS TEMPERATURE,  
e IS VAPOUR PRESSURE .

(AFTER BYRNE, 1979)

**Produced by  
School of Geography  
University of Leeds  
Leeds LS2 9JT  
From whom copies may be obtained**